CHAPTER V. PRODUCTION OF MORPHINAN ALKALOIDS IN *SACCHAROMYCES CEREVISIAE*

Abstract

The branch of benzylisoquinoline alkaloid metabolism leading to codeine and morphine includes several molecules of proven and potential pharmacological importance. Production of morphinan alkaloids in a microbial host in leu of extraction from plants will increase the availability of these molecules for drug discovery and decrease manufacturing costs. This work builds on previously engineered strains of *Saccharomyces cerevisiae* capable of converting the substrate (*R, S*)-norlaudanosoline to salutaridine, the first benzylisoquinoline alkaloid specific to the morphinan pathway. We tested the recently cloned salutaridine synthase (SalSyn) for the conversion of (*R*)-reticuline to salutaridine and compared it to CYP2D6 used in the original strains. In addition, we engineered strains to co-express salutaridine reductase (SalR) and salutaridinol-7-*O*-acetatyltransferase (SalAT) for the production of salutaridinol-7-*O*-acetate. We performed preliminary work to increase accumulation of salutaridinol-7-*O*-acetate with the end goal of developing a process for thebaine production.

5.1. Introduction

The morphinan alkaloids and their derivatives are a source of many important and diverse pharmaceuticals. Isolation from plants is the sole means of obtaining the active compounds morphine, codeine, and thebaine. Additional chemical and biosynthetic derivatization further broadens the array of useful therapeutics in this category. The goal of this work is to engineer yeast for the production of morphinan alkaloids. A microbial production host avoids rigorous purification processes and removes existing limits on plant production. Additional conversion steps can also be performed in the host organism as required. Thebaine is the initial target molecule along the morphinan branch. The requisite enzymes have been cloned, and thebaine represents only 6.5% of the total alkaloid content of *Papaver somniferum* yet can be used for the production of many semisynthetic opiate drugs[84].

Previously, the conversion of norlaudanosoline and the morphinan alkaloid salutaridine was demonstrated in yeast[4]. From salutaridine, additional downstream enzymes are available for the production of salutaridinol and salutaridinol-7-*O*-acetate (Fig. 5.1). We used a strain background constitutively expressing *Papaver somniferum* 6OMT, CNMT, and 4'OMT to convert (*R, S*)-norlaudanosoline, a commercially available substrate with the BIA backbone structure, to (*R, S*)-reticuline. Using the (*R*)- isomer of reticuline, we are able to produce salutaridine using a cytochrome P450 activity from humans or plants. This novel activity for the human CYP2D6 was demonstrated using engineered yeast cells and optimal conversion occurred in a strain background expressing a single copy of the human cytochrome P450 reductase (hCPR1). The salutaridine synthase activity (SalSyn, CYP719B) from *P. somniferum* has recently been cloned;

however, the characterization of this enzyme expressed in a recombinant host has not yet been published. We tested this enzyme in a variety of strain backgrounds and used both P450 activities in the development and initial optimization of a process for thebaine production.

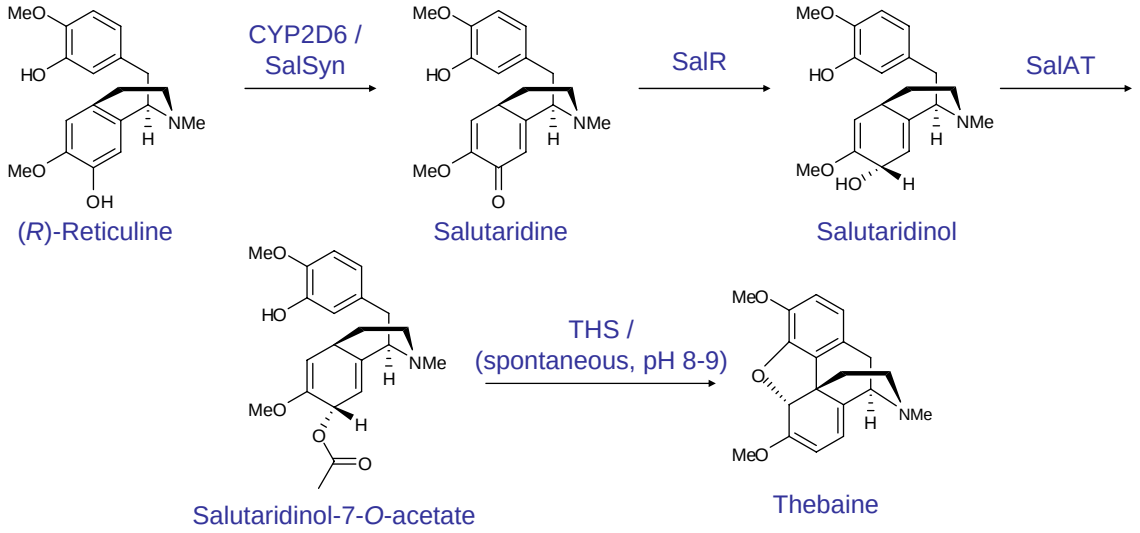

Fig. 5.1. Pathway for the production of thebaine from (*R*)-reticuline. In our engineered yeast strains, both (*R*)- and (*S*)- isomers of reticuline are produced from a racemic mixture of norlaudanosoline as the substrate for this extended branch of the pathway. Additional conversion steps by CYP2D6/SalSyn, SalR, and SalAT lead to salutaridinol-7-*O*-acetate which is spontaneously converted to thebaine at high pH and may also be facilitated by thebaine synthase (THS) in plant hosts.

The remaining steps in this pathway are catalyzed by salutaridine reductase (SalR) and salutaridinol-7-*O*-acetyltransferase (SalAT). Both enzymes have been cloned from *P. somniferum* and were tested in our yeast expression hosts. This work marks the development of a process that produces modest amounts of salutaridinol-7-*O*-acetate. However, many optimization challenges remain, primarily due to the pH dependence of thebaine formation. A two-stage process or combination of *in vivo* and *in vitro* transformations may be required.

5.2. Results

5.2.1. Expression and activity of Papaver somniferum salutaridine synthase

The recently cloned *P. somniferum* salutaridine synthase (SalSyn, CYP719B), the enzyme responsible for conversion of (*R*)-reticuline to salutaridine in plants, was codon-optimized for yeast and tested in our engineered strains. No accumulation of salutaridine was observed when this enzyme was tested in combination with the human, yeast, or *A. thaliana* P450 reductase. There are only two known P450 reductase sequences from poppy plants[85]. Unlike humans and yeast, plants are known to have multiple P450 reductase genes such that the single reductase identified from *P. somniferum* may not be the correct partner for SalSyn. We codon-optimized this sequence for the host organism *S. cerevisiae* and assembled the gene from short oligonucleotide templates. This optimized *P. somniferum* reductase was tested in combination with SalSyn. We tested the *P. somniferum* reductase on a low-copy expression vector or integrated into the host genome and were unable to observe accumulation of salutaridine from SalSyn.

We also tested various designs of SalSyn with the N-terminal sequence replaced by the first 16-18 amino acids of bovine CYP17, which has been shown to efficiently target the yeast microsomal membrane[86]. Salutaridine accumulation was not observed in these strains co-expressing the described P450 reductase partners. Although we did not observe accumulation of salutaridine attributable to SalSyn activity, we were able to show that this activity participates in the larger pathway for salutaridinol-7-*O*-acetate production and actually outperforms CYP2D6 in most strains.

5.2.2. Expression of Papaver salutaridine reductase variants for the production of salutaridinol

Additional enzymes implicated in morphine biosynthesis in plants downstream of salutaridine have been cloned and characterized. Salutaridine reductase (SalR) converts salutaridine to salutaridinol. This enzyme has been cloned from both *P. somniferum* and *P. bracteatum* species. Although the protein sequences differ by only 13 amino acids, the *P. bracteatum* variant is reportedly more stable in a bacterial host[87]. We examined protein expression levels in the W303α yeast strain and also observed higher levels of the *P. bracteatum* variant as expected (Fig. 5.2a). This variant was also shown to have more favorable catalytic properties *in vitro*[65, 87] and was therefore the initial focus of additional studies in our yeast hosts. Optimization of codon usage did not increase expression of the *P. bracteatum* SalR as observed by Western blotting experiments (Fig. 5.2a). However, this sequence was retained as increased translational efficiency is expected to reduce metabolic burden on engineered yeast strains expressing multiple recombinant proteins. Based on previous mutagenesis studies, we also constructed V106A and R48K mutants and the combinatorial mutant, which have been shown to improve turnover rate and increase NADH affinity, respectively[87]. These SalR variants were tested in combination with SalSyn and CYP2D6 (with and without SalAT) and no improvements were observed (Fig. 5.2b).

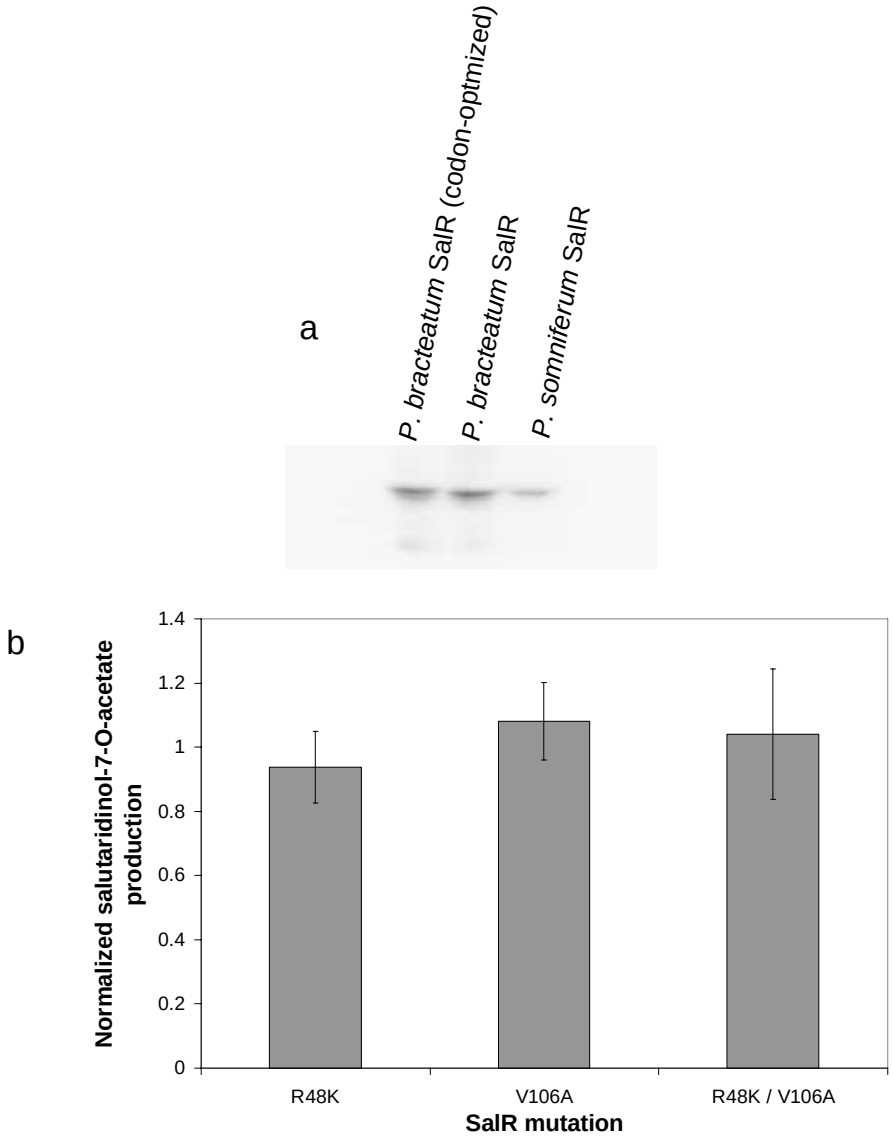

Fig. 5.2. Testing of SalR variants. **(a)** Western blotting using SalR constructs tagged with a C-terminal V5 epitope and detected with the anti-V5 HRP antibody and a chemiluminescent assay. Lanes are loaded with equal amounts of total protein from yeast lysates (50 μg). **(b)** Comparison of salutaridinol-7-*O*-acetate production by reticuline-producing yeast strains expressing yCYP2D6, SalATopt, and a SalR variant. Values are normalized to production of salutaridinol-7-*O*-acetate from a strain expressing the codon-optimized *P. bracteatum* SalR lacking any amino acid substitutions.

Identification of the salutaridinol peak proved difficult in many of our strains as it appeared as a small tail on the reticuline peak since these metabolites have the same

molecular weight. However, one strain expressing yCYP2D6 and the codon-optimized *P. bracteatum* SalR from TEF6 promoters from a high copy plasmid (pCS1605; Table 5.1) produced a clearly discernable second peak identifiable as salutaridinol by its fragmentation pattern (Fig. 5.3)[76]. We also observed a decrease but not total depletion of salutaridine. Full conversion of this substrate is unlikely since SalR is substrate inhibited at low salutaridine concentrations with a K_i of 140 μM[87]. This may also be a reason so little activity is observed in other strains even when the same *SalR* sequence is expressed. Low salutaridine production is particularly an issue when using SalSyn, but even in the case of CYP2D6 where salutaridinol is observable, it is only estimated to reach a maximum concentration of 75 μM in the growth media with a presumably similar intracellular concentration based on a passive diffusion transport mechanism for BIA molecules.

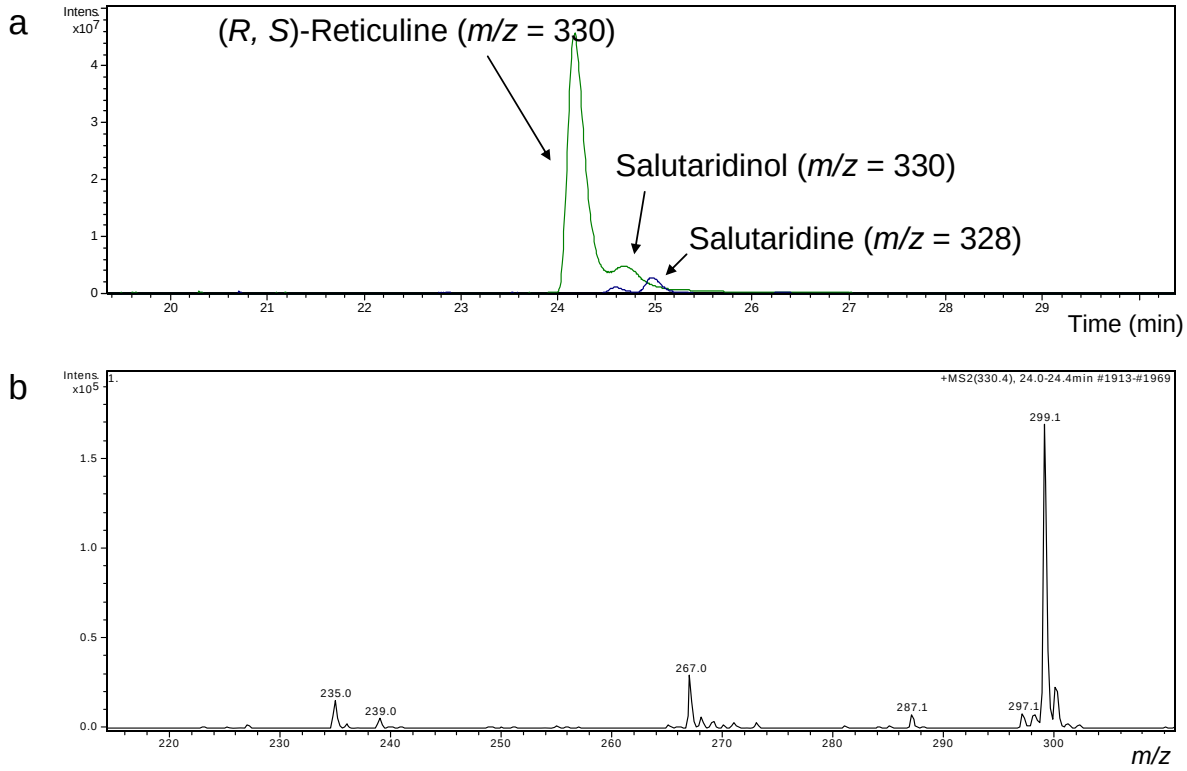

Fig. 5.3. Salutaridinol production. **(a)** Salutaridinol appears as a second peak following reticuline elution at the same molecular weight (*m/z* = 330, green). The substrate peak salutaridine is shown in blue (*m/z* = 328). **(b)** The fragmentation pattern of the peak for *m/z* = 330 at 24.4 min shows ions 299, 287, 267, and 239 that are characteristic for salutaridinol[76]. Additional ions 273, 255, and 241 are visible at higher resolution. Yeast strains not expressing SalR did not show this additional peak or this fragmentation pattern for the *m/z* = 330 ion.

SalR is also an NADPH-dependent enzyme and we suspect that cofactor limitation may be an issue as NADPH is generated in only a few endogenous reactions: the two dehydrogenase reactions of the pentose-phosphate pathway, the $NADP^+$-dependent isocitrate dehydrogenase reaction, the $NADPH^+$-dependent acetaldehyde dehydrogenase reaction, and the reaction catalyzed by malic enzyme[88]. As the flux through the pentose-phosphate pathway is tightly regulated, the shunt pathway including the mitochondrial malic enzyme was previously identified as a metabolic engineering target for creating an additional source of NADPH. Expression of a short version of

Mae1p lacking the first 90 nucleotides coding for the mitochondrial targeting sequence may be a way to increase the availability of cytosolic NADPH for the SalR reaction. We may also engineer the enzyme to have altered cofactor specificity beyond what was obtained with the R48K mutation.

5.2.3. Expression of salutaridinol-7-O-acetyltransferase and development of a process for thebaine production

The next cloned enzyme in the morphinan branch is the acetyl-CoA-dependent salutaridinol 7-*O*-acetyltransferase (SalAT) from opium poppy[89, 90]. Salutaridinol-7-*O*-acetate undergoes a subsequent spontaneous allylic elimination to form thebaine at pH 8-9. However, at pH 6-7 the product [8,9-dihydro-5H-2,12-dimethoxy-1-hydroxy-7-methyl-dibenz[d,f]azoninium]acetate is formed which can be reduced by $NaBH_4$ to neodihydrothebaine[89] (Fig. 5.4).

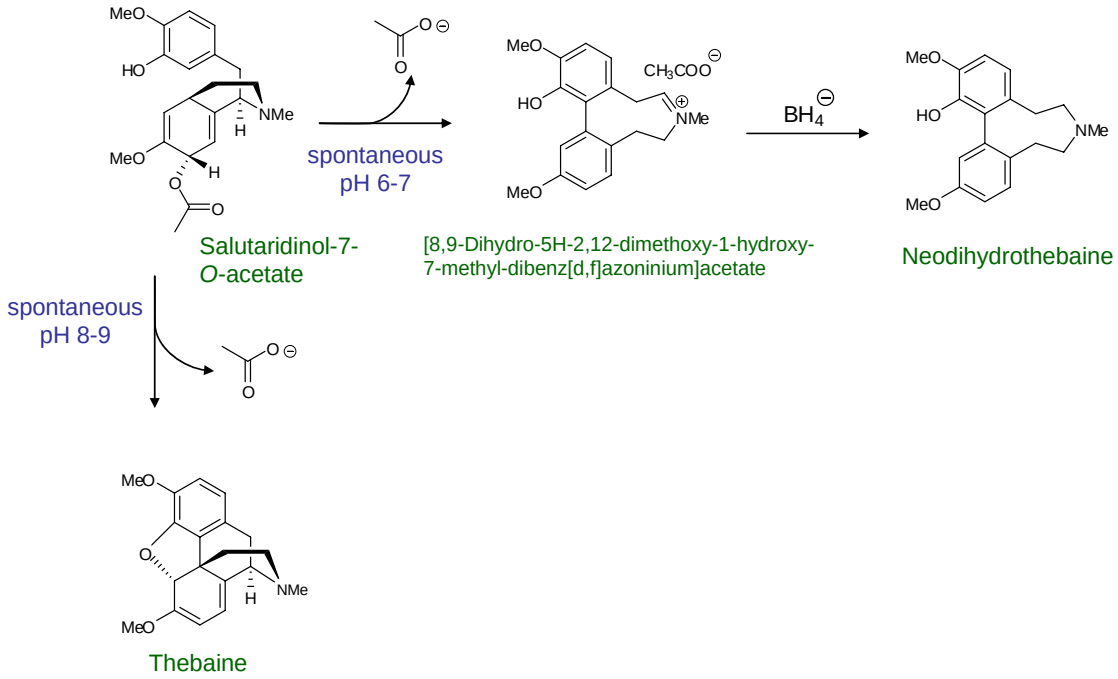

Fig. 5.4. Pathways for the formation of thebaine and neodihydrothebaine. These two very different molecules are derived from salutaridinol-7-*O*-acetate depending on pH. At pH 8-9, loss of the acetyl group leads to thebaine whereas at pH 6-7, loss of the acetyl group leads to [8,9-Dihydro-5H-2,12-dimethoxy-1-hydroxy-7-methyl-dibenz[d,f]azoninium]acetate which can be reduced to neodihydrothebaine.

A seemingly insignificant but reproducible peak was observed for salutaridinol-7-*O*-acetate when using the *P. somniferum* SalAT coding sequence in our system without additional considerations for pH optimization. This peak at *m/z* = 372 appears when using any combination of yCYP2D6 or SalSyn and *P. somniferum* or *P. bracteatum* SalR variants co-expressed with SalAT and is not present in the absence of SalAT (Fig. 5.5). There was no significant difference in salutaridinol-7-*O*-acetate accumulation observed between the various combinations of preceding enzymes tested so we sought other ways to optimize our strains.

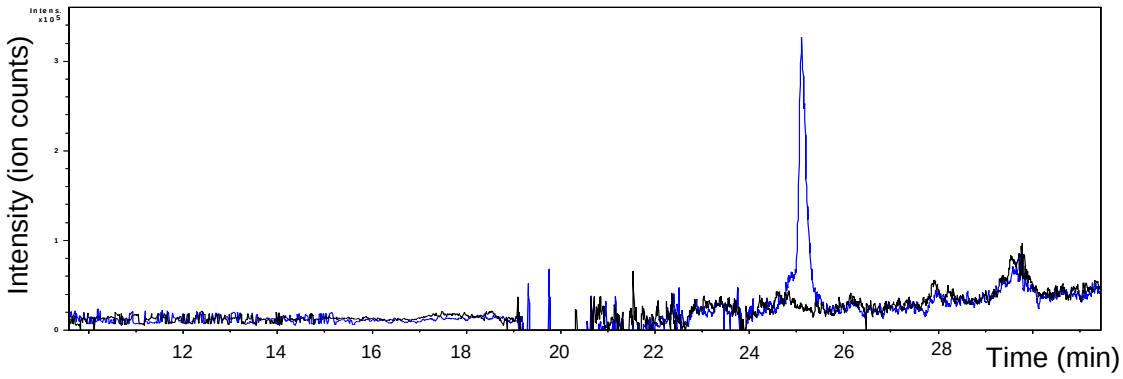

Fig. 5.5. LC-MS analysis of salutaridinol-7-*O*-acetate. Extracted ion chromatograms of *m/z* = 372 for a strain expressing yCYP2D6/hCPR1, PbSalR, and SalAT (blue) and a strain expressing yCYP2D6/hCPR1, and PbSalR only (black); both strains also express the necessary enzymes for reticuline production from norlaudanosoline. The peak identified as salutaridinol-7-*O*-acetate elutes at 25 min and co-elutes with a 313 ion consistent with the loss of the acetyl group in the mass spectrometer.

Using a construct in which the native SalAT sequence was tagged with a V5 epitope for Western blotting, no protein was observed in either the soluble fraction or aggregated with the cell pellet. Codon-optimization greatly increased expression of SalAT in our *S. cerevisiae* strains (Fig. 5.6a).

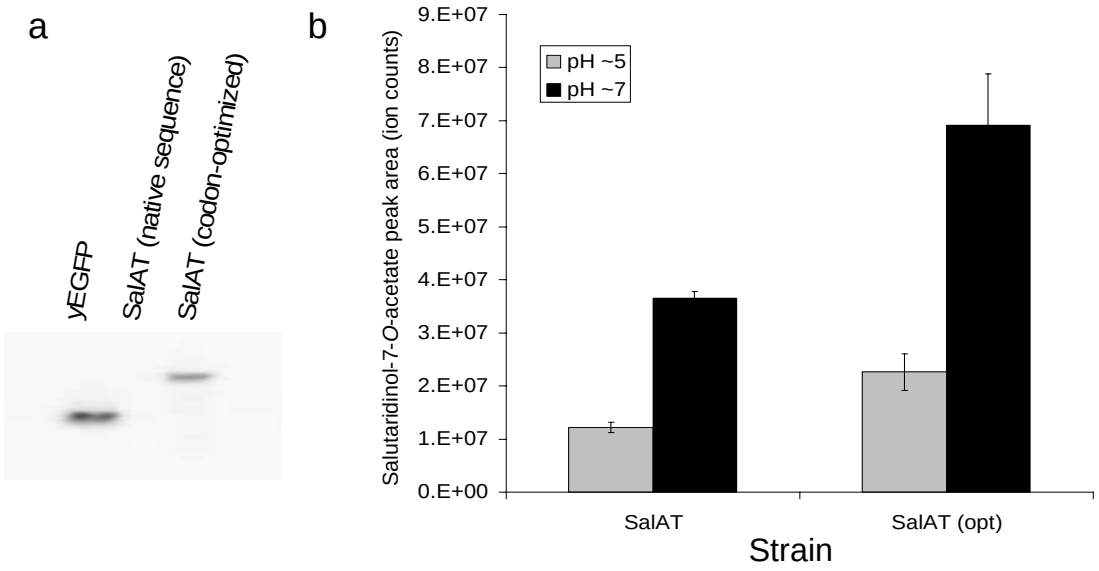

Fig. 5.6. Codon-optimization increases SalAT expression. **(a)** Western blot of SalAT constructs tagged with a C-terminal V5 epitope and incubated with the anti-V5 HRP antibody for chemiluminescent detection. Expression of SalAT using the native sequence is not observed, but the codon-optimized SalAT is expressed at levels comparable to a highly-expressed yEGFP. Lanes are equally loaded with 50 μg total protein. **(b)** Comparison of salutaridinol-7-*O*-acetate production from strains expressing SalSyn/AtATR, PsSalR, and either SalAT or the codon-optmized SalAT (CSY514 and CSY515). Cultures were grown at pH ~5 (standard synthetic complete media; grey) or buffered to maintain pH ~7 with 10 mM phosphate buffer (black).

Once expression was improved, enzymatic activity *in vivo* still remained a major hurdle with little observable increase in salutaridinol-7-*O*-acetate production. The K_m for salutaridinol is relatively low at 9 μM[90] but still may be limiting in our system in addition to acetyl-CoA requirements. Furthermore, the pH optimum for SalAT is 7-9 with a temperature optimum of 47ºC[90]. These are far from yeast physiological conditions of pH

~5 and 30ºC. Yeast cells are also more adaptable to acidic rather than alkaline pH, and only yeast strains evolved to be thermotolerant tend to grow at temperatures approaching or exceeding 37°C. It was quickly demonstrated that yeast cells inoculated into unbuffered media at pH 8 were able to grow but the alkaline pH was not maintained, and growth was severely retarded in media buffered to maintain the pH at 8. Other enzymatic activities, specifically CYP2D6, were also compromised at pH > 7. However, at pH ~7, cell viability is not noticeably impaired and we observed an increase in salutaridinol-7-*O*-acetate accumulation up to 3-fold in several of our strains (Fig. 5.6b and 5.7b). At this higher pH, we were also able to discern a significant difference between strains expressing SalSyn versus CYP2D6. Strains expressing SalSyn accumulated ~2-fold more salutaridinol-7-*O*-acetate compared to strains expressing CYP2D6, indicating that SalSyn has higher activity when functioning as part of the larger pathway (Fig. 5.7).

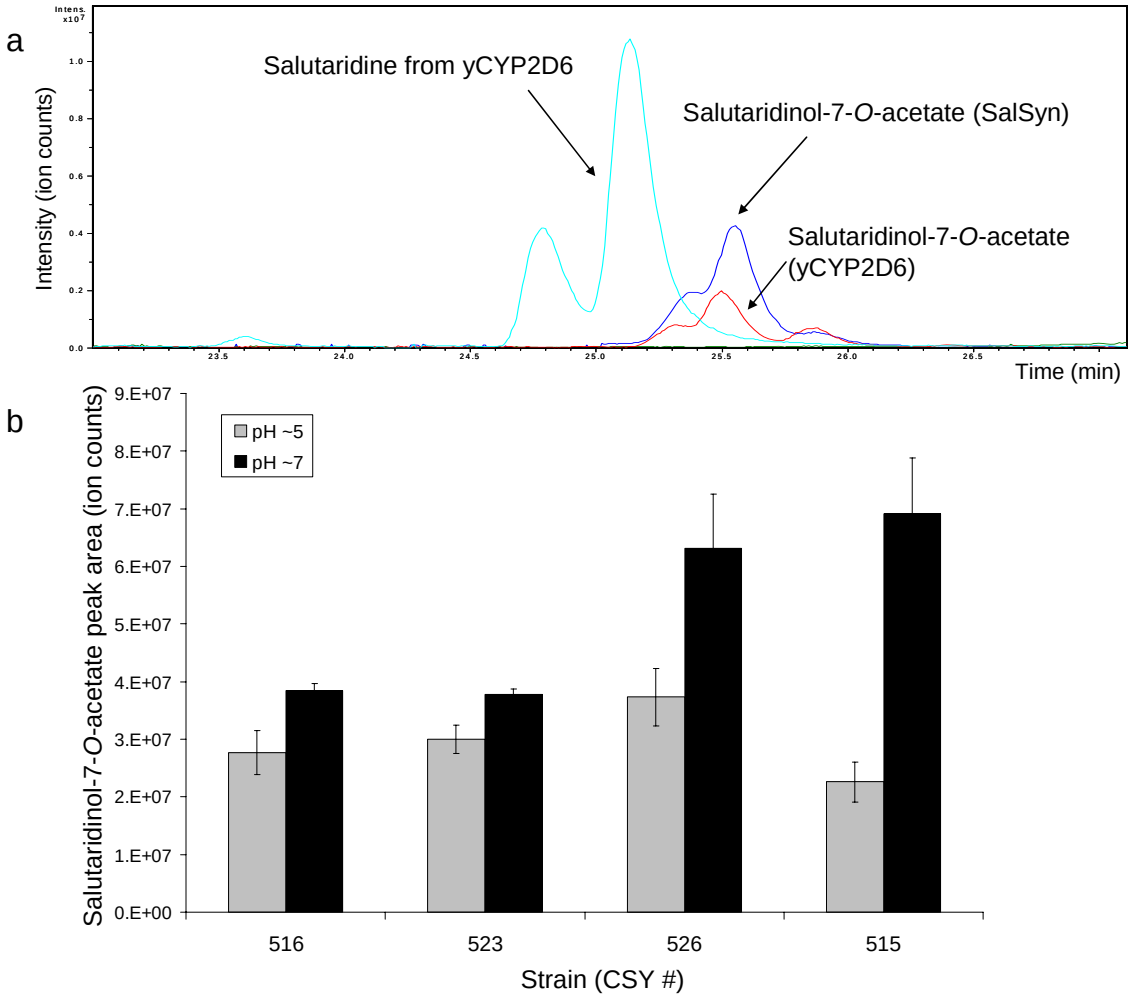

Fig. 5.7. Comparison of CYP2D6 and SalSyn for salutaridinol-7-*O*-acetate production. **(a)** Extracted ion chromatograms of salutaridine (*m/z* = 328; cyan) and salutaridinol-7-*O*-acetate (*m/z* = 372; red) from CSY523 expressing CYP2D6/hCPR1, PsSalR, and PsSalAT(opt); and salutaridine (*m/z* = 328; green, no peak) and salutaridinol-7-*O*-acetate (*m/z* = 372; blue) from CSY515 expressing SalSyn/AtATR1, PsSalR, and PsSalAT(opt). **(b)** Comparison of salutaridinol-7-*O*-acetate peak areas of strains expressing CYP2D6/hCPR1 and PbSalR or PsSalR (CSY516 and CSY523) and strains expressing SalSyn/AtATR. Data from cultures grown at pH ~5 (grey) and pH ~7 (black) are shown.

Based on this data, we chose to revisit SalSyn and optimization of the reductase partner using production of salutaridinol-7-*O*-acetate as a benchmark. The best SalR variant proved to be the original *P. somniferum* sequence (Fig. 5.7b), and this was used in combination with the codon-optimized SalAT to test various strain backgrounds with no

reductase or an integrated copy of AtATR1, hCPR1, or PsCPR1 behind the TEF1 promoter (Fig. 5.8a). We also found that one design with the N-terminal signal sequence replaced by that of bovine CYP17 outperformed the native SalSyn (Fig. 5.8b).

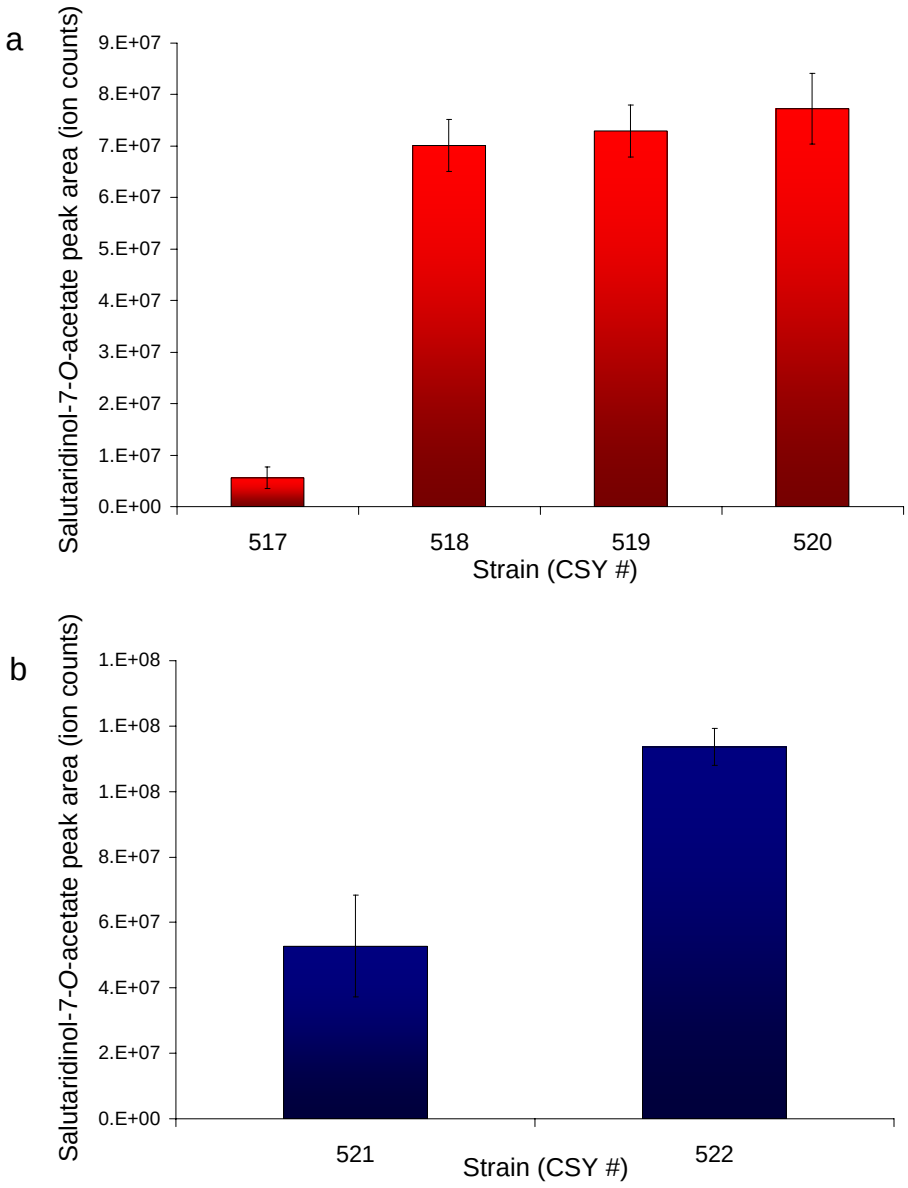

Fig. 5.8. Comparison of SalSyn reductase partners and signal sequences. **(a)** Salutaridinol-7-*O*-acetate production from strains expressing SalSyn, PbSalR, and PsSalAT (opt) along with no reductase partner (CSY517), hCPR1 (CSY518), AtATR1 (CSY519), or PsCPR (CSY520). **(b)** Salutaridinol-7-*O*-acetate production from strains expressing PsCPR, PsSalR, and either the native SalSyn sequence (CSY521) or a version of SalSyn with the first 12 amino acids replaced by the bovine CYP17 16 amino acid N-terminal signal sequence.

Although we are seeing salutaridinol-7-*O*-acetate accumulation, we would like to push this towards thebaine production which should proceed spontaneously at pH 8-9. Based on the proposed mechanism, it appears that a histidine in the active site stabilizes the leaving group and can determine the preferred location of nucleophilic attack while the molecule is still bound to SalAT such that the pH at the time of reaction is critical. Our own experimental evidence also shows that increasing the pH following the growth phase does not alter the ratio of salutaridinol-7-*O*-acetate to thebaine. We therefore sought a two-stage process in which the cells could grow and produce other intermediates up to salutaridinol shown to accumulate at physiological pH. SalAT could then be expressed along with a simultaneous increase in pH. Rather than use a promoter that requires addition of an exogenous inducer such as GAL1 or CUP1, we examined the HSP30 promoter which was shown to be induced as the cells entered stationary phase. This allows automatic induction of SalAT as the expression levels of other enzymes expressed from constitutive promoters are declining (Fig. 5.9a).

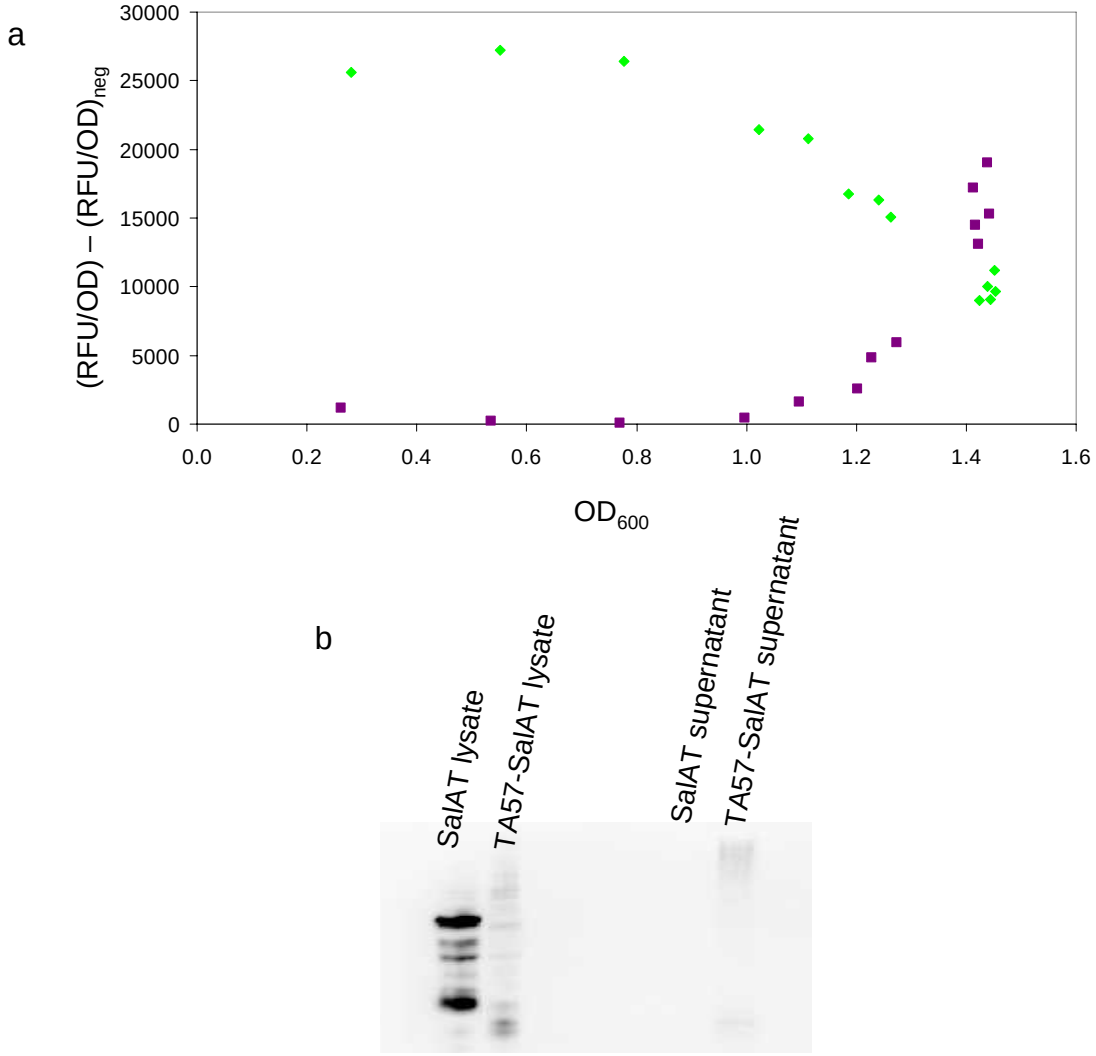

Fig. 5.9. Alternative promoter and signal sequence for SalAT. **(a)** Time course data of P_{TEF1}:yEGFP (green diamonds) and P_{HSP30}:yEGFP (purple squares). As the cells reach stationary phase, the TEF1 promoter expression decreases while the HSP30 promoter turns on. Relative fluorescence and OD_{600} were measured in a 96-well plate format and normalized to a negative control with no yEGFP expression. **(b)** Western blot of yeast lysates (50 µg total protein) and supernatants concentrated ~250-fold, 20 µl loaded. Expression and localization of the yeast codon-optimized SalAT is compared to the same coding sequence with a TA57 leader sequence for processing through the secretory pathway.

In addition, we looked at secretion of SalAT since the intracellular pH does not necessarily correspond to the extracellular pH which is much easier to measure and manipulate. The modified α-factor leader sequence in which the C-terminus was

modified from “SLDKR” so “SMAKR” was tested as well as the TA57 leader sequence lacking N-linked glycosylation sites. The spacer sequences were EEAEAEAEPK and EEGEPK, respectively[91]. We analyzed the growth media of a yeast strain expressing a tagged version of the secreted SalAT to examine protein levels (Fig. 5.9b). Intracellular TA57-SalAT levels were low although little protein was detected in the concentrated growth media. This could be due in large part to proteolysis either before or after the culture was harvested.

We tested each of these SalAT constructs in a reticuline-producing strain background also expressing P_{TEF1}*:hCPR1* from the chromosome, and P_{TEF6}*:yCYP2D6* and P_{TEF6}*:PbSalR* from a high-copy plasmid. For constructs expressing SalAT from the HSP30 promoter, phosphate buffer was added to increase the pH to ~7.5 as the cells entered stationary phase, typically following ~24 h growth in the presence of substrate. Constitutive SalAT constructs were tested at physiological pH or buffered to pH 7-7.5 upon backdilution in the presence of substrate.

For secreted enzymes, no salutaridinol-7-*O*-acetate production was observed under any pH conditions. This could be attributable to low or incorrect expression of the secreted enzymes or inactivity of SalAT in the growth media due to lack of acetyl-CoA or other factors. For the SalAT lacking a signal sequence, salutaridinol-7-*O*-acetate production was greater when using a strong constitutive promoter compared to the HSP30 promoter. It is unclear whether this is related to differences in expression levels between the HSP30 and TEF6 promoters or the timing of induction and pH change.

Further investigations into the mechanism of SalAT and thebaine formation are necessary for the rational engineering of improved yeast strains. While we are able to

accumulate more salutaridinol-7-*O*-acetate at pH 7 without severely compromising growth, yeast are not tolerant to more alkaline pH and higher temperatures. Even if we were to evolve such a robust strain, preceding enzymatic activities may suffer.

It is also possible that acetyl-CoA is limiting, in which case, previous studies have shown that this pool can be increased for use in a heterologous pathway[92]. Using the work engineering the pyruvate dehydrogenase bypass as a guide, we plan to construct strains to overexpress both the *S. cerevisiae ALD6* and the *Salmonella acs* L641P mutant. It is important to note that overexpression of *ALD6* may also increase the NADPH pool for the SalR enzyme activity.

Many of the strains we constructed for salutaridinol-7-*O*-acetate production, in the hopes of producing thebaine, accumulated similar levels of the precursor. However, one clear trend was that the combination of all *P. somniferum* enzymes was superior although CYP2D6 produced more salutaridine and *P. bracteatum* SalR produced more salutaridinol. This result, along with RNAi studies in plants, suggests the existence of protein-protein interactions[93, 94]. Specifically, in opium poppy, depletion of SalAT results in accumulation of salutaridine rather than salutaridinol, indicating that both SalR and SalAT are required for production of salutaridinol[93]. In addition, overexpression of SalAT in plants resulted in increased morphine, codeine, and thebaine production, indicating that SalAT is limiting in the native pathway[93]. In our recombinant host, it is unclear whether the lack of other poppy proteins is limiting the flux to thebaine. If metabolon formation including additional uncloned genes (which may have undesired products) is an issue, it is unclear how to get around this in our host organism. One strategy is testing of variants from other organisms, particularly those known to

accumulate thebaine such as *P. bracteatum*. Other engineering and evolutionary strategies remain to be seen.

5.3. Discussion

The morphinan alkaloids represent an important branch of BIA metabolites of interest to the pharmaceutical industry. This work marks the first effort towards the development of a microbial host to perform the final conversion steps leading to thebaine production. We successfully demonstrated conversion of the commercially available substrate norlaudanosoline to salutaridinol-7-*O*-acetate, the precursor to thebaine, building upon a previously characterized yeast strain background[4]. In our best strains, we are able to achieve ~7-8% conversion of reticuline which is estimated to correspond to salutaridinol-7-*O*-acetate titers of up to 15 mg l^{-1}. We also attempted to optimize the activity of the recently-cloned SalSyn (CYP719B) and were unable to observe salutaridine accumulation although the presence of downstream metabolites indicated that this enzyme is functional in our host strains. Further optimization of this first step using the native plant enzyme SalSyn may alleviate the bottleneck in this pathway. Additional optimization of SalR and SalAT activities may also be required to develop a viable process for production of these molecules. This could be through engineering yeast strains with increased cofactor pools and/or engineering the proteins themselves to have higher activity under physiological conditions. We did observe strains expressing all *P. somniferum* enzyme variants to have the greatest accumulation of salutaridinol-7-*O*-acetate. This is not terribly surprising given previous plant studies indicating protein interactions are required for activity[93, 94]. Moreover, the lack of expression of additional

downstream enzymes may also limit the flux through this pathway if indeed they are required for complete metabolon formation and function. Finally, the sequencing of a thebaine synthase (THS) activity from one or more BIA producing plants and its incorporation into our yeast hosts may facilitate conversion of salutaridinol-7-*O*-acetate to thebaine under physiological conditions.

5.4. Materials and Methods

5.4.1. Plasmid and yeast strain construction

We obtained restriction enzymes, T4 DNA ligase, and other cloning enzymes from New England Biolabs. We performed polymerase chain reaction (PCR) amplifications using Expand High Fidelity PCR System (Roche). Oligonucleotide synthesis was performed by Integrated DNA Technologies. A list of engineered yeast strains and plasmids is provided (Table 5.1).

We used standard molecular biology techniques to construct the BIA expression vectors[59]. BIA expression constructs contained the 2μ high-copy yeast origin of replication along with appropriate yeast selection markers and ampicillin resistance. Recombinant enzymes were expressed from the yeast TEF1 promoter and flanked by a CYC1 terminator sequence. We constructed shuttle vectors for subcloning of 1 or 2 cDNA sequences in this fashion. The cDNA sequences for the native *P. somniferum* SalR, *P. somniferum* SalAT, and yeast codon-optimized SalSyn were synthesized by DNA2.0. The *P. bracteatum* SalR sequence was obtained through a series of site directed mutagenesis reactions to make the necessary 13 amino acid substitutions in the *P. somniferum* SalR sequence (QuikChange II, Stratagene). The codon-optimized sequences

for *P. bracteatum* SalR, *P. somniferum* SalAT, and *P. somniferum* CPR were designed using GeneDesigner software (DNA2.0) and assembled using primers designed by DNAWorks2.4 (Center for Information Technology, National Institutes of Health).

We transformed ligation reactions into an electrocompetent *E. coli* strain, DH10B (Invitrogen; F-*mcr*A Δ(*mrr-hsd*RMS-*mcr*BC) ϕ80d*lac*ZΔM15 Δ*lac*X74 *deo*R *rec*A1 *end*A1 *ara*D139 Δ (*ara, leu*)7697 *gal*U *gal*K λ-*rps*L *nup*G), using a Gene Pulser Xcell System (BioRAD) according to the manufacturer's instructions. We conducted plasmid isolation using the Wizard Plus SV Minipreps DNA purification system (Promega) according to the manufacturer's instructions. Subcloning was confirmed by restriction analysis and sequence verification (Laragen, Inc.). We transformed plasmids into the appropriate *S. cerevisiae* strains using a standard lithium acetate protocol[62]. All yeast strains used in this work were based on the haploid yeast strain W303α (MATα *his3-11,15 trp1-1 leu2-3 ura3-1 ade2-1*)[63]. *E. coli* cells were grown on Luria-Bertani media (BD Diagnostics) with 100 μg/ml ampicillin (EMD Chemicals) for plasmid maintenance, and *S. cerevisiae* cells were grown in synthetic complete media (BD Diagnostics) supplemented with the appropriate dropout solution for plasmid maintenance (Calbiochem).

Table 5.1. Engineered yeast strains and plasmids.

Strain	Plasmid(s)	Integrated constructs	Plasmid-based constructs
CSY288		*his3*::P_{TEF1}-*Ps6OMT*, *leu2*::P_{TEF1}-*PsCNMT*, *ura3*::P_{TEF1}-*Ps4'OMT*	
CSY409		*his3*::P_{TEF1}-*Ps6OMT*, *leu2*::P_{TEF1}-*PsCNMT*, *ura3*::P_{TEF1}-*Ps4'OMT*, *trp1*::P_{TEF1}-*AtATR1*-*loxP*-Kan^R	
CSY488		*his3*::P_{TEF1}-*Ps6OMT*, *leu2*::P_{TEF1}-*PsCNMT*, *ura3*::P_{TEF1}-*Ps4'OMT*, *trp1*::P_{TEF1}-hCPR-*loxP*-*LEU2*	
CSY506		*his3*::P_{TEF1}-*Ps6OMT*, *leu2*::P_{TEF1}-*PsCNMT*, *ura3*::P_{TEF1}-*Ps4'OMT*, *trp1*::P_{TEF1}-PsCPR(opt)-*loxP*-*LEU2*	
CSY514	pCS1357, pCS1449	*his3*::P_{TEF1}-*Ps6OMT*, *leu2*::P_{TEF1}-*PsCNMT*, *ura3*::P_{TEF1}-*Ps4'OMT*, *trp1*::P_{TEF1}-*AtATR1*-*loxP*-Kan^R	P_{TEF1}-*PsSalR*, P_{TEF1}-*PsSalAT*, P_{TEF1}-*SalSyn*
CSY515	pCS1449, pCS1540	*his3*::P_{TEF1}-*Ps6OMT*, *leu2*::P_{TEF1}-*PsCNMT*, *ura3*::P_{TEF1}-*Ps4'OMT*, *trp1*::P_{TEF1}-*AtATR1*-*loxP*-Kan^R	P_{TEF1}-*PsSalR*, P_{TEF1}-*PsSalATopt*, P_{TEF1}-*SalSyn*
CSY516	pCS1480, pCS1507	*his3*::P_{TEF1}-*Ps6OMT*, *leu2*::P_{TEF1}-*PsCNMT*, *ura3*::P_{TEF1}-*Ps4'OMT*, *trp1*::P_{TEF1}-hCPR-*loxP*-*LEU2*	P_{TEF1}-*PbSalR*, P_{TEF1}-*PsSalAT*, P_{TEF6}-*yCYP2D6*
CSY517	pCS1558, pCS1507	*his3*::P_{TEF1}-*Ps6OMT*, *leu2*::P_{TEF1}-*PsCNMT*, *ura3*::P_{TEF1}-*Ps4'OMT*	P_{TEF1}-*PbSalR*, P_{TEF1}-*PsSalATopt*, P_{TEF1}-*CYP17-SalSynB*
CSY518	pCS1558, pCS1507	*his3*::P_{TEF1}-*Ps6OMT*, *leu2*::P_{TEF1}-*PsCNMT*, *ura3*::P_{TEF1}-*Ps4'OMT*, *trp1*::P_{TEF1}-hCPR-*loxP*-*LEU2*	P_{TEF1}-*PbSalR*, P_{TEF1}-*PsSalATopt*, P_{TEF1}-*CYP17-SalSynB*
CSY519	pCS1558, pCS1507	*his3*::P_{TEF1}-*Ps6OMT*, *leu2*::P_{TEF1}-*PsCNMT*, *ura3*::P_{TEF1}-*Ps4'OMT*, *trp1*::P_{TEF1}-*AtATR1*-*loxP*-Kan^R	P_{TEF1}-*PbSalR*, P_{TEF1}-*PsSalATopt*, P_{TEF1}-*CYP17-SalSynB*
CSY520	pCS1558, pCS1507	*his3*::P_{TEF1}-*Ps6OMT*, *leu2*::P_{TEF1}-*PsCNMT*, *ura3*::P_{TEF1}-*Ps4'OMT*, *trp1*::P_{TEF1}-PsCPR(opt)-*loxP*-*LEU2*	P_{TEF1}-*PbSalR*, P_{TEF1}-*PsSalATopt*, P_{TEF1}-*CYP17-SalSynB*
CSY521	pCS1449, pCS1540	*his3*::P_{TEF1}-*Ps6OMT*, *leu2*::P_{TEF1}-*PsCNMT*, *ura3*::P_{TEF1}-*Ps4'OMT*, *trp1*::P_{TEF1}-PsCPR(opt)-*loxP*-*LEU2*	P_{TEF1}-*PsSalR*, P_{TEF1}-*PsSalATopt*, P_{TEF1}-*SalSyn*
CSY522	pCS1558, pCS1540	*his3*::P_{TEF1}-*Ps6OMT*, *leu2*::P_{TEF1}-*PsCNMT*, *ura3*::P_{TEF1}-*Ps4'OMT*, *trp1*::P_{TEF1}-PsCPR(opt)-*loxP*-*LEU2*	P_{TEF1}-*PsSalR*, P_{TEF1}-*PsSalATopt*, P_{TEF1}-*CYP17-SalSynB*
CSY523	pCS1480, pCS1540	*his3*::P_{TEF1}-*Ps6OMT*, *leu2*::P_{TEF1}-*PsCNMT*, *ura3*::P_{TEF1}-*Ps4'OMT*, *trp1*::P_{TEF1}-hCPR-*loxP*-*LEU2*	P_{TEF1}-*PsSalR*, P_{TEF1}-*PsSalATopt*, P_{TEF1}-*yCYP2D6*
CSY526	pCS1449, pCS1507	*his3*::P_{TEF1}-*Ps6OMT*, *leu2*::P_{TEF1}-*PsCNMT*, *ura3*::P_{TEF1}-*Ps4'OMT*, *trp1*::P_{TEF1}-*AtATR1*-*loxP*-Kan^R	P_{TEF1}-*PbSalR*, P_{TEF1}-*PsSalATopt*, P_{TEF1}-*SalSyn*
	pCS1508		P_{TEF6}-*yCYP2D6*, P_{TEF6}-*PsSalATopt*
	pCS1554		P_{TEF1}-*PbSalRopt*
	pCS1605		P_{TEF6}-*yCYP2D6*, P_{TEF6}-*PbSalRopt*
	pCS1606		P_{TEF6}-*PsSalATopt*
	pCS1607		P_{HSP30}-*PsSalATopt*
	pCS1608		P_{HSP30}-α*PsSalATopt*
	pCS1609		P_{HSP30}-*TA57-SalATopt*

5.4.2. Cell growth conditions

For metabolite assays, overnight cultures of yeast cells were grown to stationary phase and backdiluted 1:20 into 2-3 ml fresh media plus the appropriate substrate, typically norlaudanosoline or laudanosoline added from a 20 mM stock to a final concentration of 4 mM. For buffered cultures, 0.1 M phosphate at pH 8.0 was added as a 10X stock to yield a final pH of ~7 which was maintained during cell growth. The concentration of yeast nitrogen base, ammonium sulfate, amino acids, and dextrose were adjusted so that the final concentration was consistent with standard media conditions. Cells were grown ~48 hr for most assays such that stationary phase was reached to allow for more consistent and reproducible results. No significant difference was observed if cells were grown for an additional 2-4 days.

5.4.3. Analysis of metabolite production

We evaluated BIA metabolite levels by LC-MS/MS analysis of cell extracts and growth media. At appropriate time points, aliquots of yeast cultures were centrifuged to recover cells as pellets and allow collection of the growth media. We analyzed the growth media or an appropriate dilution directly by LC-MS/MS. Samples were run on an Agilent ZORBAX SB-Aq 3 x 250 mm, 5 μm column with 0.1% acetic acid as solvent A and methanol as solvent B. We used a gradient elution to separate the metabolites of interest as follows: 0-10 min at 100% A, 10-30 min 0-90% B, 30-35 min 90-0% B, followed by a 5 min equilibration at 100% A between samples. Following LC separation, metabolites were injected into an Agilent 6320 ion trap MSD for detection and identification. We verified chromatogram data through at least three independent experiments and from multiple strains where appropriate. Quantification of metabolites was based on the integrated area of the extracted ion chromatogram peaks[64] calculated using DataAnalysis for 6300 Series Ion Trap LC/MS Version 3.4 (Bruker Daltonik GmbH) and reported as the mean ± s.d. When appropriate, we normalized the measured levels to a metabolite peak of known concentration in the growth media.

5.4.4. Analysis of protein levels through Western blotting

We constructed plasmids for Western blotting experiments by cloning the C-terminal epitope tag(s) from pYES-NT/A (Invitrogen) into our standard TEF1 expression vector followed by subcloning of the enzyme of interest. We transformed individual plasmids into wild-type yeast cells using a standard lithium acetate protocol. Overnight cultures were grown and backdiluted 1:100 into 100 ml cultures. Cells were grown to OD_{600} ~1.5 and pelleted by centrifugation. The media was removed and cells were washed in 1 ml PBS, pelleted, and resuspended in 0.5 ml Y-PER plus HALT protease

inhibitor (Pierce). Cells were vortexed for ~20 min and the lysate separated by centrifugation. We estimated total protein using the Coomassie Plus Protein Assay Reagent (Pierce) and loaded ~50 μg of each sample onto a protein gel. We used NuPage 4-12% Bis-Tris gels with MES running buffer and transfer buffer according to the manufacturer's instructions (Invitrogen). Proteins were blotted onto a nitrocellulose membrane (Whatman) using a semi-dry transfer cell (Bio-Rad) for 25 min at 25 V. We incubated the membrane with the Anti-V5 HRP antibody (Invitrogen) according to the manufacturer's instructions (Invitrogen) with 5% BSA as the blocking agent. Proteins were detected with the West Pico Super Signal Detection kit (Pierce) and imaged on a ChemiDoc XRS system (Bio-Rad).

5.4.5. Fluorescence quantification

For measurements of HSP30 and TEF1 promoter activity using a fluorescent reporter, overnight cultures were grown in synthetic complete media with 2% dextrose and backdiluted 1:100 into fresh media to begin the time course assay. We measured fluorescence (excitation 485 nm, emission 515 nm) and OD_{600} values on a fluorescence plate reader (TECAN, Safire) at various time points between 4 and >48 hr. Fluorescence values were normalized using the OD_{600} reading and values from a no stain control (wild-type cells) were subtracted.